

Structural aspects of corrosion resistance in alloys based on the Fe₃Al intermetallic phase in the cast state

M. M. LACHOWICZ^{1*}, K. HAIMANN¹, M. B. LACHOWICZ¹, R. JASIONOWSKI², S. PAWLAK³

¹Institute of Materials Science and Applied Mechanics, Wrocław University of Technology,
Smoluchowskiego 25, 50-372 Wrocław, Poland

²Institute of Basic Technical Sciences, Maritime University of Szczecin, Podgórna 51-53, 70-205 Szczecin, Poland

³Institute of Metallurgy and Material Science, Polish Academy of Sciences, Reymonta 25, 30-095 Kraków, Poland

This paper presents the results of investigation of four cast alloys based on the Fe₃Al intermetallic phase. Microstructure tests using light microscopy, electron scanning microscopy and X-ray diffraction methods, have been performed. On this basis, a presence of particles rich in zirconium and molybdenum, and in case of the alloy with 28 at.% aluminium and 5 at.% chromium – the presence of sigma phase (FeCr), has been found. Also, the results of the study of the microstructure influence on the electrochemical corrosion resistance in the 5 % NaCl solution have been presented. The Fe-26Al-2Cr-1Mo-0.1Zr-0.005B at.% and Fe-26Al-5Cr-1Mo-0.1Zr-0.005B at.% alloys exhibited increased corrosion resistance in comparison to the Fe-23Al-1Mo-0.1Zr-0.005B at.% alloy without chromium addition. The appearance of the sigma phase in the alloy of Fe-28Al-5Cr-1Mo-0.1Zr-0.005B at.% chemical composition resulted in lowering the corrosion resistance of this alloy and a change in corrosion character from the pitting to the intercrystalline one.

Keywords: *Fe₃Al based iron aluminides, microstructure, electrochemical corrosion, sigma phase*

© Wrocław University of Technology.

1. Introduction

In recent years a significant interest in the materials based on intermetallic phases, including the Fe-Al composition alloys, has been observed. It has been related to their outstanding resistance to high-temperature corrosion, while keeping the low density [1, 2]. Research works are being conducted in parallel to find the other potential applications of these alloys [3–8].

The structure of the alloys in the intermetallic phase matrix depends on aluminium content. Within the range of 36 to 51 at.% Al, the ordered FeAl phase (structure B2), and in the range of 23 to 35 at.% – the Fe₃Al phase (structure DO3) are stable. Because of the technological difficulties appearing in plastic working of these alloys, elements are searched for to enhance the process of shaping the alloys by plastic working [1,

2]. Moreover, the alloys show good ability for solution consolidation [1]. One of the most frequently used alloy elements, which influences the phenomenon of phase ordering in the Fe-Al alloys, is chromium [9]. It has been found that chromium, similarly to molybdenum, affects the increase in corrosion resistance in these alloys [4].

In terms of microstructure, addition of chromium initiates the development of the Fe-Al-Cr system phases in these alloys. In the two-component Al-Cr diagram six intermediate equilibria phases appear: Al₇Cr, Al₁₁Cr₂, Al₄Cr, Al₉Cr₄, Al₈Cr₅, and AlCr₂ [10]. In the iron alloys containing chromium, a σ phase of the approximate stoichiometric formula FeCr may appear, due to separation from the solid solution at a temperature of 815 °C. This is the intermetallic phase crystallizing in a tetragonal lattice, whose cell contains 30 atoms. Theoretically, it should contain 47 at.% of chromium, however in practice chromium content ranges from 43 to 50 at.%, and

*E-mail: marzena.lachowicz@pwr.wroc.pl

therefore it forms a secondary solid solution [11]. σ phases are hard and brittle and their occurrence in alloys is very unfavourable, because it increases their brittleness and lowers their corrosion resistance.

There are only few literature reports related to electrochemical corrosion resistance of alloys at the intermetallic phase matrix. So far, the electrochemical corrosion studies of the Fe-Al based alloys have shown, that corrosion rate of the iron aluminides is independent of the crystal structure but the alloy in the ordered states B2 or DO3 has a higher pitting resistance than the alloy in disordered states [4]. The corrosion rate of the Fe₃Al-type alloy in a chloride-containing solution is very low. The uniform corrosion penetrations is less than 0.2 mm/year and the behaviour observed in the chloride containing solution for this intermetallics is very similar to that of the 316L stainless steel [3, 4]. In the work [6] it has been shown that the resistance to corrosion of the alloys in the FeAl phase matrix is essentially influenced by the aluminium content and the type of the corrosion solution applied.

The aim of the studies performed was the analysis of the influence of aluminium and chromium content on the microstructure of the alloys in the Fe₃Al intermetallic phase matrix in the as-cast state, in the 5 % NaCl water solution.

2. Research methodology

2.1. Materials

The studied materials were: Fe-23Al-1Mo-0.1Zr-0.005B at.%, Fe-26Al-2Cr-1Mo-0.1Zr-0.005B at.%, Fe-26Al-5Cr-1Mo-0.1Zr-0.005B at.%, and Fe-28Al-5Cr-1Mo-0.1Zr-0.005B at.% alloys in the as-cast state. The material was obtained by melting a batch of pure elements in the Balzers type vacuum induction oven, in the temperature of 1500 °C and in the vacuum of 2.66–6.66 Pa.

Because of the constant content of molybdenum, boron and zirconium in the studied alloys, to simplify the notation, only aluminium

and chromium content will be given in the further part of this work.

2.2. Test methodology

The research was conducted using light microscopy with a NEOPHOT 32 microscope, and scanning electron microscopy (SEM SE, EDX) with a JEOL-JSM 6610A microscope coupled with a X-ray microanalyser JEOL-EX 230, after etching a sample in 50 % CH₃COOH + 33 % HNO₃ + 17 % HCl solution.

The phase analysis was performed using the X-ray diffraction method with a Brücker D-8 Discover diffractometer, equipped with an open Euler circle and “polycap” type optics.

Electrochemical direct-current measurements used for evaluating the corrosion resistance were conducted by the measurement of the open-circuit potential. The $i = f(E)$ relationship during the polarization tests in the three-electrode measuring circuitry was recorded. The fully automated measurement system consisted of a measuring vessel, an ATLAS 0531 ELECTROCHEMICAL UNIT & IMPEDANCE ANALYSER potentiostat, and a computer controller. The auxiliary electrode was made of austenitic steel, and as a reference, the saturated Ag/AgCl electrode was applied. Samples for the corrosion tests were ground and then polished directly before the measurement. The surface of the tested electrode (sample) was equal to 0.785 cm². Surface roughness of the sample measured by means of PGM-1C profilographometer ranged from 0.01 to 0.015 μm . Before the test, each sample was immersed for 30 min. into the 5 % solution of NaCl at the temperature of 20 °C, and next it was subjected to polarization, in the same solution, in the anodic direction with the rate of $dE/dt = 1 \text{ mV/s}$. The initial value of the potential was determined on the basis of the open-circuit potential value E_o , assuming the value lower by about 200 mV. The values of corrosion current density I_{corr} , corrosion potential E_{corr} , and polarization resistance R_p were determined from the measured potential of anodic-cathodic passage at the potential increase rate of 1 mV/s, using the Stern method.

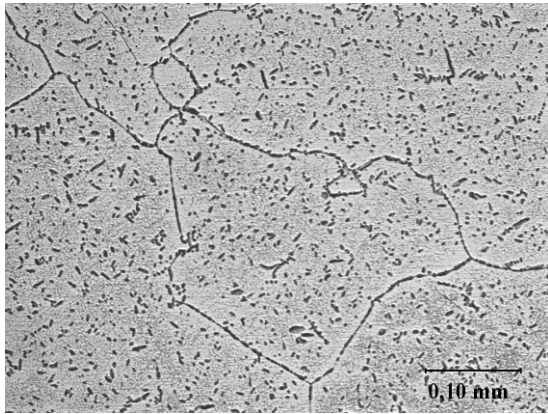


Fig. 1. Microstructure characteristic of the Fe-23Al, Fe-26Al-2Cr, Fe-26Al-5Cr alloys. Secondary solid solution (bright) with the phase precipitates on the grain boundaries and inside the grains (dark) can be recognized. Etched state. Light microscopy.

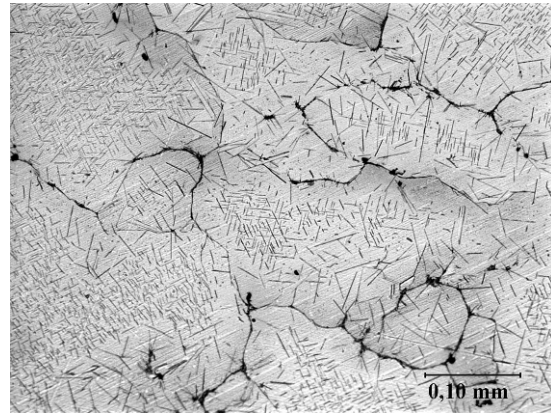


Fig. 2. Microstructure of the Fe-28Al-5Cr alloy in the cast state. Acicular particles inside the grains and on the grain boundaries (dark) of the solid solution (bright) can be recognized. Etched state. Light microscopy.

3. Results

3.1. Light microscopy

As a result of the microscopic studies it has been found that the tested alloys have a structure consisting of the secondary solid solution with visible phase precipitates inside the grains and on the grain boundaries (Fig. 1). The microscopic tests conducted for the Fe-28Al-5Cr alloy have shown the presence of acicular particles appearing inside the grains and at their boundaries. Precipitates of this type have been observed only for this type of alloy (Figs. 2-3).

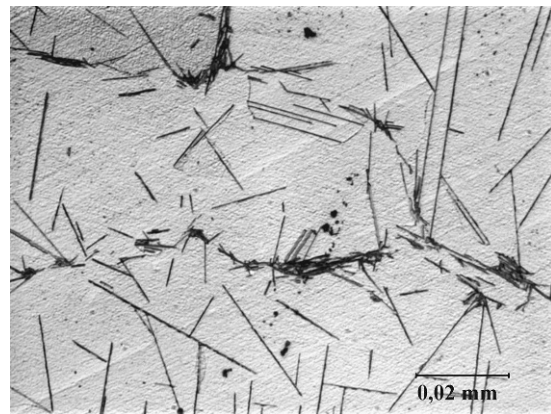


Fig. 3. Microstructure of the FeAl28Cr5 alloy in the as-cast state. Magnified fragment of the area from Fig. 2. Etched state. Light microscopy.

3.2. Scanning Electron Microscopy, SEM

The chemical composition analysis performed using the X-ray microanalyser coupled with the scanning electron microscope have shown that the fine precipitates observed in all alloys are rich in zirconium and molybdenum (Figs. 4, 5). Moreover, the presence of very fine borides or nitrides of zirconium of a regular shape, inside the solid solution grains, have been found.

The research made using the electron microscopy has shown that within the grain boundaries the acicular precipitates appearing in

the Fe-28Al-5Cr alloy created eutectics with the secondary solid solution (Figs. 6, 7).

The microanalysis of chemical composition of the particles observed in the alloy microstructure with the highest aluminium and chromium content (Fe-28Al-5Cr) has shown the increased chromium and iron content compared to the matrix (Fig. 8). Their chemical composition and acicular character indicate the creation of the σ phase in these alloys, unfavourable for their mechanical and corrosion properties.

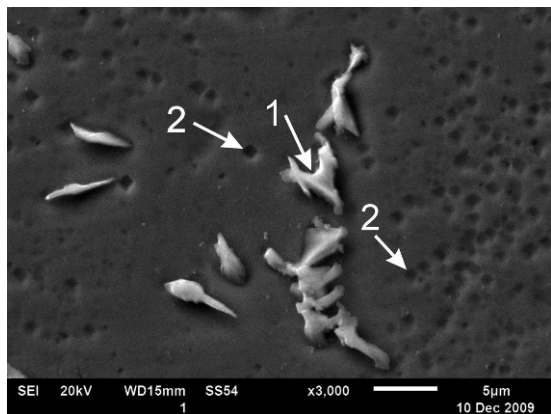


Fig. 4. Microstructure of the Fe-23Al alloy. The arrows indicate bright precipitates of a phase rich in zirconium and molybdenum (1), very fine particles of zirconium nitrides and borides (2) at the background of the secondary solid solution (Fe,Cr)₃Al. Etched state. SEM.

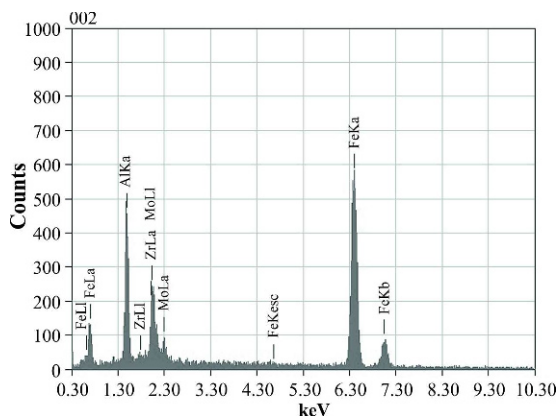


Fig. 5. Spectrum of the characteristic X-ray radiation from the particle shown in Fig. 4

3.3. X-ray diffraction

Research made using the X-ray diffraction method has confirmed that the matrix of the studied alloys was the secondary solid solution based on the intermetallic phase Fe₃Al, crystallizing in the regular face-centered (Fm3m) lattice. Taking into account that chromium could replace the iron atoms it is quite obvious that the diffraction pattern shows better correlation with the Fe₂CrAl phase having the same crystallographic lattice.

In the diffraction pattern of the Fe-28Al-5Cr alloy, two reflexes of low intensity, appearing at

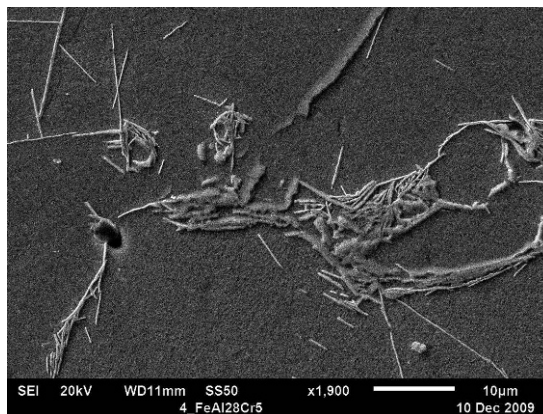


Fig. 6. Microstructure of the Fe-28Al-5Cr alloy in the as-cast state. Etched state. SEM.

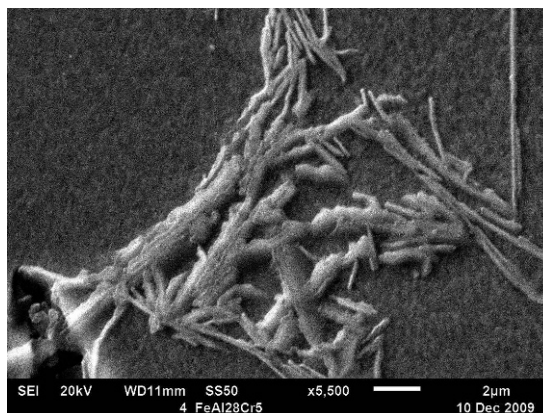


Fig. 7. Microstructure of the Fe-28Al-5Cr alloy in the as-cast state. Etched state. SEM.

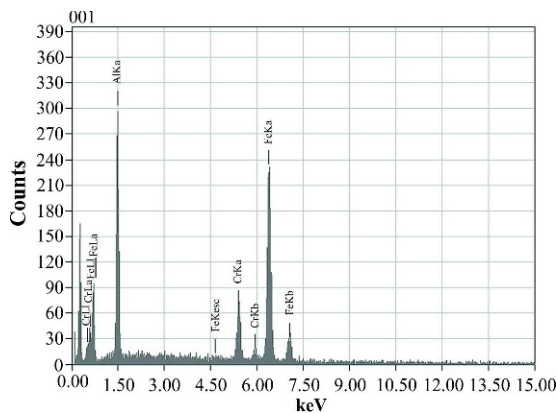


Fig. 8. Spectrum of the characteristic X-ray radiation from the particles shown in Fig. 7.

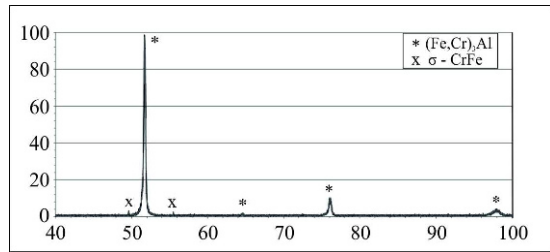


Fig. 9. An example of X-ray diffraction pattern for the Fe-28Al-5Cr alloy.

the 2θ angle equal to 49.56 and 55.17° , have been observed. It has been found that they come from the σ phase (FeCr), crystallizing in the tetragonal lattice, and their low intensity is related to relatively low content of the analysed phase in the alloy (Fig. 9). The appearance of the peaks coming from this phase in the obtained X-ray diffractogram confirms the earlier hypothesis based on microscopic observations.

3.4. Electrochemical tests

As a result of the electrochemical tests made in 5 % NaCl solution, it has been found that all the tested alloys in the cast state were characterized by the negative value of the corrosion potential, E_{corr} . In the case of alloys containing chromium in their chemical composition, such as Fe-26Al-5Cr and Fe-28Al-2Cr, an increase in the corrosion resistance, as compared to the Fe-23Al alloy, was observed. It was manifested by the shift in the corrosion potential E_{corr} towards the higher values, as well as lowering the corrosion currents in the cathodic and anodic parts of the polarisation curves (polarogram) for these alloys. Moreover, the lowering of the polarization resistance value R_p , responsible for the corrosion rate, to the lowest value obtained for these alloys, has been found. The alloys had similar microstructure, which confirms the observations presented in the literature [4], that chromium dissolved in a matrix enhances the corrosion resistance of these alloys. An example of potentialdynamic curves obtained for the tested alloys is shown in Fig. 10. The average electrochemical parameters: E_o (open-circuit potential), E_{corr} (corrosion

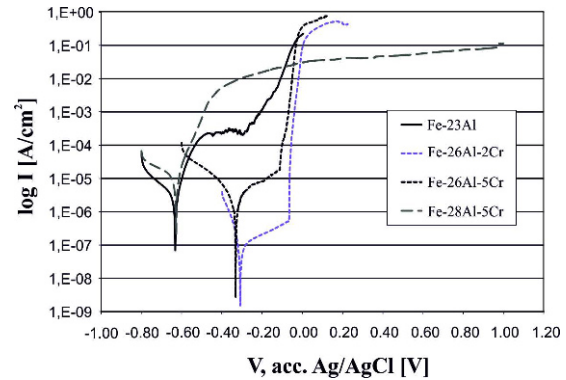


Fig. 10. An example of potentialdynamic curves for the tested alloys.

Table 1. Electrochemical parameters obtained for the tested alloys.

Sample	E_0 [mV]	E_{corr} [mV]	I_{corr} [$\mu\text{a}/\text{cm}^2$]	R_p [$\text{k}\Omega\cdot\text{cm}^2$]
Fe-23Al	-617	-622	91.13	1350.7
Fe-26Al-2Cr	-262	-318	1.37	98.4
Fe-26Al-5Cr	-245	-293	1.12	19.7
Fe-28Al-5Cr	-649	-634	10.58	933.6

potential), I_{corr} (corrosion current density), as well as R_p (polarization resistance) coming from three measurements of the tested alloys have been presented in Table 1.

It has been found that in the Fe-28Al-5Cr alloy, with the highest total content of aluminium and chromium, i.e. 28 at.% and 5 at.%, correspondingly, a drop in corrosion resistance in the as-cast state was probably caused by the development of sigma phase (FeCr). The alloy demonstrated the values of the E_{corr} and I_{corr} close to those of the Fe-23Al alloy. In the case of this alloy a rapid increase in the corrosion currents density was observed in the anodic part of the curve, directly after exceeding the corrosion potential E_{corr} . The process slowed down at about -0.4 V potential, after the sample got coated with a layer of oxide (Fig. 12).

Polarization resistance R_p reached its highest value for the alloy free of chromium. The drop of R_p value for the Fe-26Al-2Cr and Fe-26Al-5Cr

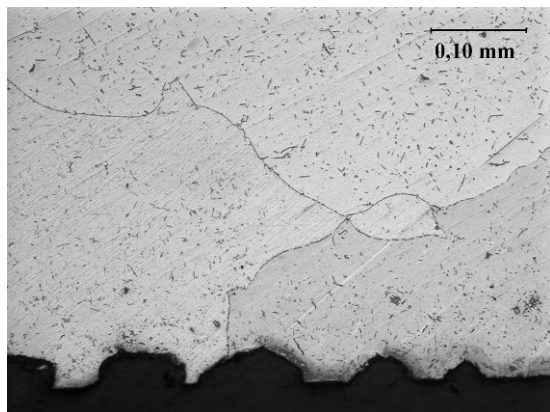


Fig. 11. Sample cross-section of the Fe-23Al alloy after electrochemical tests. Pitting corrosion is visible. Light microscopy. Etched state.

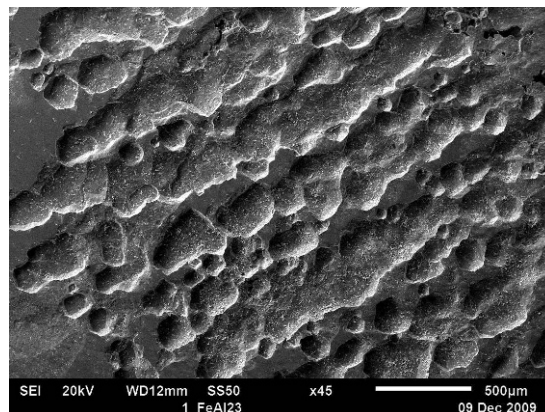


Fig. 12. Surface of the Fe-23Al alloy after electrochemical tests. Pitting type corrosion is visible. SEM.

alloys and a subsequent rise of this parameter was associated with the development of the sigma phase in the microstructure (Table 1).

3.5. Microscopic study after corrosion tests

Microscopic observations made directly after electrochemical tests have shown that in the case of Fe-23Al, Fe-26Al-2Cr and Fe-26Al-5Cr alloys, the surface of the samples was covered with corrosion pits of crater type, appearing both on the grain boundaries and inside the grains (Figs. 11, 12). In the case of Fe-26Al-2Cr and Fe-26Al-5Cr alloys, which contained chromium, it has been found that the shape of the pits was more irregular in comparison to the chromium-free alloy Fe-23Al, leading to the creation of characteristic “tunnels” in the bulk material (Fig. 13).

The process of matrix dissolving led to revealing a phase rich in zirconium and molybdenum. This confirms its cathodic character in relation to the matrix (Fig. 14). The nature of the attack in the Fe₃Al based intermetallics after subjecting it to anodic polarisation in 5 % NaCl solution is illustrated in Fig. 14, which shows the crystallographic grain structure inside the pit.

In the case of Fe-28Al-5Cr alloy, a change in corrosion type from the pitting one to the mainly intercrystalline was discovered (Fig. 15).

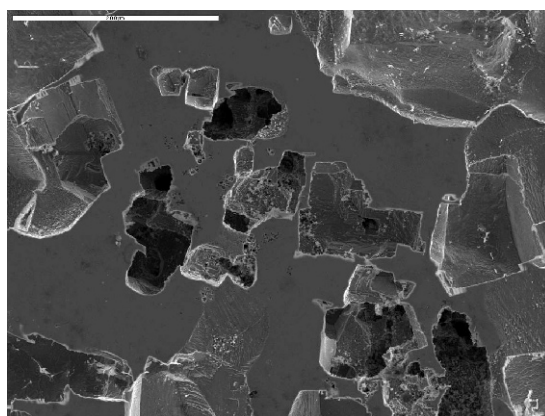


Fig. 13. Pitting corrosion created at the Fe-26Al-5Cr alloy surface after electrochemical tests. SEM.

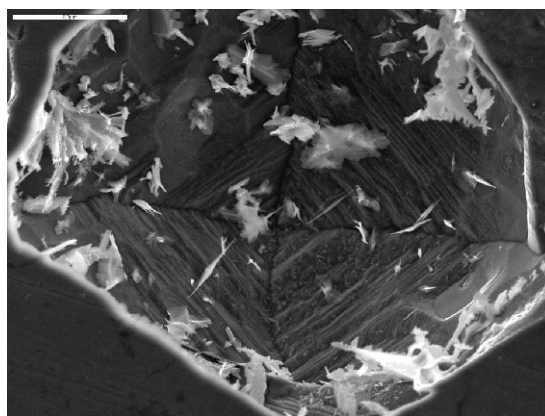


Fig. 14. Surface of the Fe-23Al alloy after electrochemical tests. Micrograph of an ordered Fe₃Al alloy shows the crystallographic nature of the pit formation. SEM.

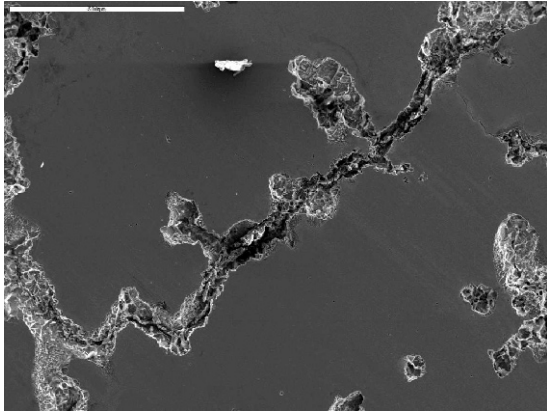


Fig. 15. Sample surface after corrosion tests of the Fe-28Al-5Cr alloy in the as-cast state. Visible corrosion located within grain boundaries. SEM.

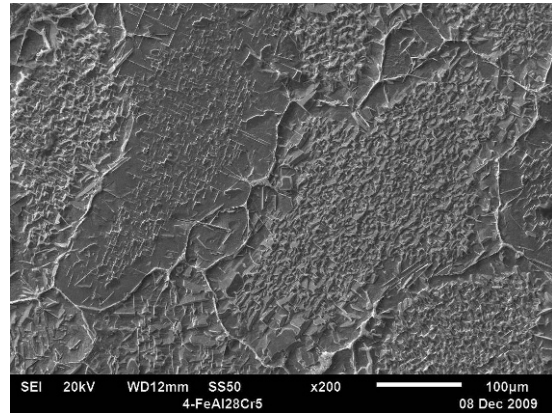


Fig. 16. Sample surface after corrosion tests of the Fe-28Al-5Cr alloy in the as-cast state. Visible solid solution dissolution, leading to revealing the σ phase precipitations. SEM.

On the basis of microscopic studies performed for the samples after corrosion tests, an obvious dissolving of grain boundaries was found (Fig. 15) at the sites where the separation occurred on the grain boundaries. However, corrosion damage appeared also inside the grains. Dissolving of the secondary solid solution on the base of Fe_3Al phase has revealed the acicular particles of the σ phase present in the microstructure of this alloy (Figs. 16–20). As a consequence, accumulation of this phase on the grain boundaries led to locating corrosion mainly within these areas. This testifies a strong cathodic character of these precipitates in relation to the matrix (Fig. 19). The precipitates appearing within a grain displayed a columnar character with a sharp shape (Fig. 20).

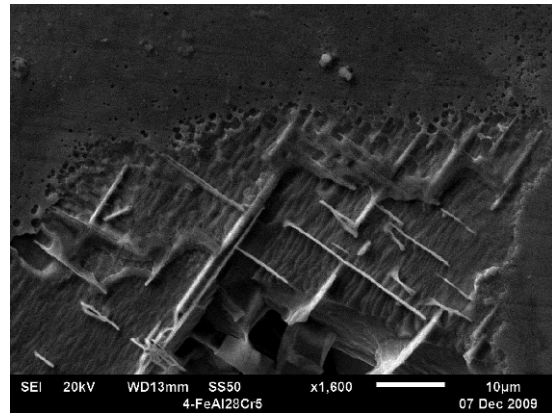


Fig. 17. Sample surface after corrosion tests of the Fe-28Al-5Cr alloy in the as-cast state. Local matrix dissolution, leading to revealing the σ phase (FeCr) precipitations is visible. SEM.

4. Conclusions

The microscopic studies of alloys in the as-cast state have shown that their matrix is constituted by the secondary solid solution composed mainly of intermetallic phase Fe_3Al . Due to the presence of chromium in its chemical composition, the obtained diffraction pattern showed better correlation with the Fe_2CrAl phase of the same lattice.

In the microstructure of the studied alloys, the particles rich in zirconium and molybdenum,

appearing inside the grains and on their boundaries, were observed. In the case of the alloy with aluminium content equal to 28 at.%, and the highest chromium content used in this study, creation of the acicular σ phase (FeCr) inside the grains and at their boundaries was observed.

In the literature concerning the subject, the influence of particular elements on the corrosion resistance of the alloys based on the Fe-Al system has been analysed [4–8]. However, the attention was mainly focused on the high-temperature corrosion resistance of these alloys. The knowledge

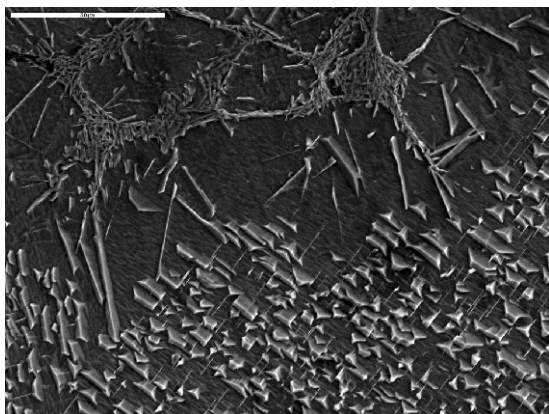


Fig. 18. Sample surface after corrosion tests of the FeAl28Cr5 alloy in the as-cast state. The σ phase (FeCr) particles is revealed as a result of the matrix dissolution. SEM.

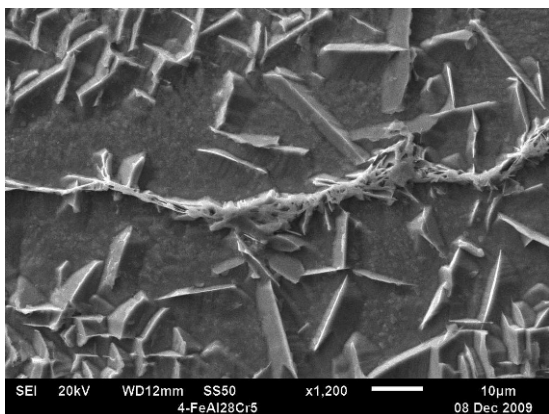


Fig. 19. Sample surface after corrosion tests of the Fe-28Al-5Cr alloy in the as-cast state. The σ phase precipitates appearing within the grains and creating eutectics with the solid solution on the grain boundaries, revealed as a result of matrix dissolution. SEM.

of the electrochemical characteristics of these alloys may extend their application range. In [6] it has been shown that in the environment containing chloride ions, the higher corrosion resistance was displayed by the alloys with a lower aluminium content. Based on the research conducted in this work, an increase in corrosion resistance of Fe-26Al-2Cr and Fe-26Al-5Cr alloys in the as-cast state in comparison to the Fe-23Al alloy was observed. All three alloys had similar microstructure, which indicated that chromium,

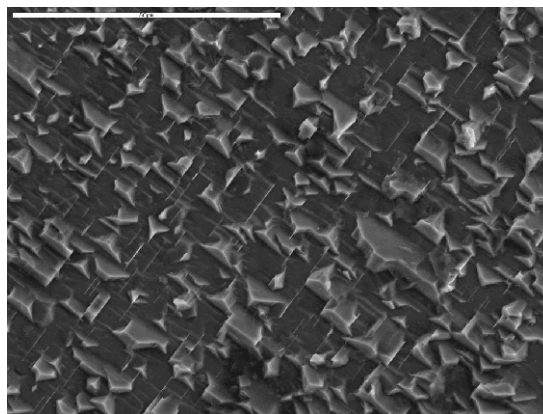


Fig. 20. Sample surface after corrosion tests at the Fe-28Al-5Cr alloy in the as-cast state. Characteristic columnar precipitates of the σ phase appearing within the grains can be recognized. SEM.

while dissolving in the matrix, increased the electrochemical corrosion resistance of these alloys. This was also testified by the more favourable course of corrosion curves obtained for the Fe-26Al-5Cr alloy in comparison to the Fe-26Al-2Cr alloy. The achieved results confirm the literature data, which indicate a positive influence of Cr on corrosion behaviour of alloys at the intermetallic phase matrix of the Fe-Al system [4].

In this work the alloys with both chromium and aluminium content were tested in 5 % water solution of NaCl. It was shown that in the case when the both elements are contained in the chemical composition, their effect on corrosion resistance is not linear. When the total content of chromium and aluminum in the primary structure is high, the σ phase (FeCr) may occur. The appearance of the σ in cathodic phase with respect to matrix, in the alloy with the highest total content of aluminium and chromium, i.e. 28 and 5 at.% respectively, resulted in worsening the corrosion resistance of the Fe-28Al-5Cr alloy in the as-cast state. The alloy showed the values of E_{corr} and I_{corr} close to that of Fe-23Al alloy, not containing chromium in its chemical composition. At the same time, exclusively for this alloy, a rapid growth in corrosion current density was observed directly

after exceeding the corrosion potential. The process slowed down when a layer of oxide on the sample surface was created. The polarization resistance R_p , inversely proportional to the corrosion rate, reached the highest value for the alloy free of chromium. This value dropped for the Fe-26Al-2Cr and Fe-26Al-5Cr alloys but the appearance of σ (FeCr) phase in the microstructure caused a subsequent rise in the R_p parameter.

Microscopic studies conducted using the scanning electron microscopy method have shown that, in the case of the Fe-28Al-5Cr alloy, also the type of corrosion has changed from the pitting to the intercrystalline one. It was related to appearance of the σ phase clusters at the solid solution boundaries.

Acknowledgements

Dr. Eng. Marzena Lachowicz is a scholarship holder of the Minister of Science and Higher Education for prominent young scientists.

References

- [1] PALM M., *Intermetallics*, 13 (2005), 1286.
- [2] BOJAR Z., PRZETAKIEWICZ W., *Materiały metalowe z udziałem faz międzymetalicznych*, Publishing House BELStudio, Warszawa, 2006 (in Polish).
- [3] GARCIA-ALONSO M.C., LOPEZ M.F., ESCUDERO M.L., GONZALEZ-CARRASCO J.L., MORRIS D.G., *Intermetallics*, 7 (1999), 185.
- [4] SHANKAR RAO V., *Electrochim. Acta*, 9 (2004), 4533.
- [5] CEBULSKI J., LALIK S., MICHALIK R., *J. Achiev. Mater. Manuf. Eng.*, 16 (2008), 15.
- [6] CEBULSKI J., MICHALIK R., LALIK S., *J. Achiev. Mater. Manuf. Eng.*, 16 (2006), 40.
- [7] CEBULSKI J., MICHALIK R., LALIK S., *J. Achiev. Mater. Manuf. Eng.*, 18 (2006), 59.
- [8] GONZALEZ-RODRIGUEZ J.G., GONZALEZ-CASTANEDA M., CUELLAR-HERNANDEZ M., DOMINGUEZ-PATINO G., ROSAS G., *J. Solid State Electr.*, 12 (2008), 707.
- [9] FROMMEYER G., JIMENEZ S.A., DERDER C., *Z. Metallkd.*, 90 (1999), 930.
- [10] MURRAY J.L., *J. Phase Equilib.*, 19 (1998), 368.
- [11] MIKIKITS-LEITNER A., SEPIOL B., LEITNER M., CIESLAK J., DUBIEL S., *Phys. Rev. B*, 82 (2010), 100101(1).

Received 2010-09-27

Accepted 2012-07-08